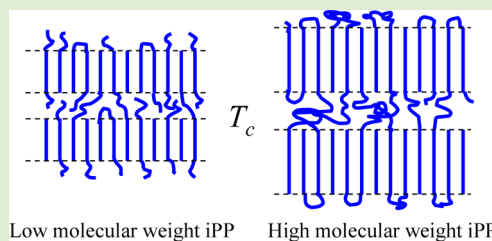


Molecular Weight Dependency of Surface Free Energy of Native and Stabilized Crystallites in Isotactic Polypropylene

Ying Lu, Yaotao Wang, Zhiyong Jiang, and Yongfeng Men*

State Key Laboratory of Polymer Physics and Chemistry, Changchun Institute of Applied Chemistry, Chinese Academy of Sciences, University of Chinese Academy of Sciences, Renmin Street 5625, 130022 Changchun, People's Republic of China

ABSTRACT: Two isotactic polypropylene samples were investigated to study the influence of molecular weight on the crystallization and melting behaviors via temperature-dependent small-angle X-ray scattering techniques. In a phase diagram of inverse lamellar thickness and temperature, the crystallization and melting behaviors can be described by two linear dependencies of different slopes and different limiting temperatures at infinite crystalline lamellar thickness. The slope of the crystallization line depends on the surface free energy of the just formed native crystallites, whereas that of the melting line is linked to the surface free energy of stabilized ones. The two polypropylene samples showed different crystallization lines and melting lines, indicating strong changes in surface free energies of the native as well as stabilized crystallites. Such changes are consequences of changes in molecular conformation during crystallization for samples with different molecular weights. Indeed, the low molecular weight sample crystallizes extensively into an extended-chain conformation, whereas the high molecular weight one ends up with normal folded-chain crystallites.



Different from small molecular or oligomer systems, crystallization of polymers from their molten state normally yields stacked lamellar crystallites separated by entangled amorphous phase. The thickness of the resulting lamellar crystallites is usually much smaller than the corresponding radius of gyration of the polymer chain. Therefore, to understand crystallization behavior of polymers, it is essential to consider differences and similarities between small molecules and polymers during crystallization. Indeed, such studies exist that molecular weight had been an important parameter in considering crystallization of polymers. In general, typical investigations were conducted in polymers of polyethylene (PE),^{1–3} isotactic polypropylene (iPP),^{4,5} polybutene-1 (PB-1),^{6–9} as well as poly(tetramethyl-p-silphenylene)siloxane,¹⁰ and so on. These discoveries had proved that different morphologies of chains in crystallites were presented as varying the molecular weight, for example, both of PE^{1,3} and PB-1,⁷ chains existed as the state either of folded-chain or of extended-chain in crystallites. And then, the surface free energy of crystallites σ_e , which is associated with the molecular weight, could be affected by the state of chains in crystallites. According to the experiments completed by Mandelkern et al.,^{1,3} σ_e increased with increasing of molecular weight in PE. This finding was interpreted as the fact that extended-chain crystallites were formed in the lower molecular weight samples while crystallites with folded-chain were more preferable to be produced as molecular weight increased. It is apparent that the interfacial region is much less crowded and distorted in lower molecular weight PE exhibiting extended-chain crystallites, whereas a crowded and packed in a distorted surface region is expected in the higher molecular weight PE samples due to their folded-chain crystallites nature.³ Therefore, with further lateral growth more chains can be brought into this surface

region in higher molecular weight PE, and thus, a higher σ_e was expected in order to promote crystalline growth.³

Meanwhile, the dependency of molecular weight on the melting behavior also revealed some unexpected results. Such as the findings in iPP, Yamada et al.⁵ declared a contrary conclusion described as the surface free energy decreased with increased molecular weight due to the influence of chain ends. They illustrated that the lower molecular weight sample owned much more chain ends leading to a higher surface free energy. Besides, the same tendency of surface free energy variation with molecular weight in iPP was also pointed out by Cheng.⁴ For the first sight, it seems contradictory that opposite relationships between surface free energy of crystalline lamellae and the molecular weight were given in different systems. However, for a further consideration, these disagreements could be reasonably resolved by a crystallization theory recently proposed by Strobl^{11,12} that the crystallization and melting in polymers are not reversible processes. A diagram of crystallization and melting lines expressed by the crystallization temperature T_c and the melting point T_m to the reverse crystalline thicknesses d_c^{-1} were depicted in separate lines. Hence, the surface free energies referred to native crystallites in the crystallization process and stable crystallites in melting procedure¹¹ may be different. Based on these results, further experiments by using two iPPs of very different molecular weights to explore the effect of molecular weight on the crystallization and melting processes via time- and temperature-dependent small-angle X-ray scattering (SAXS) and differential scanning calorimeter (DSC) techniques were implemented in

Received: September 18, 2014

Accepted: October 10, 2014

Published: October 14, 2014

the current work. The two samples with different molecular weights exhibited two separate crystallization lines and melting lines with an opposite tendency of changes in the slope of the lines as a function of molecular weight, indicating different molecular weight dependencies of surface free energy in native and stabilized crystallites in iPP.

Figure 1 registered the DSC melting curves of the two iPP samples after isothermal crystallization at settled temperatures.

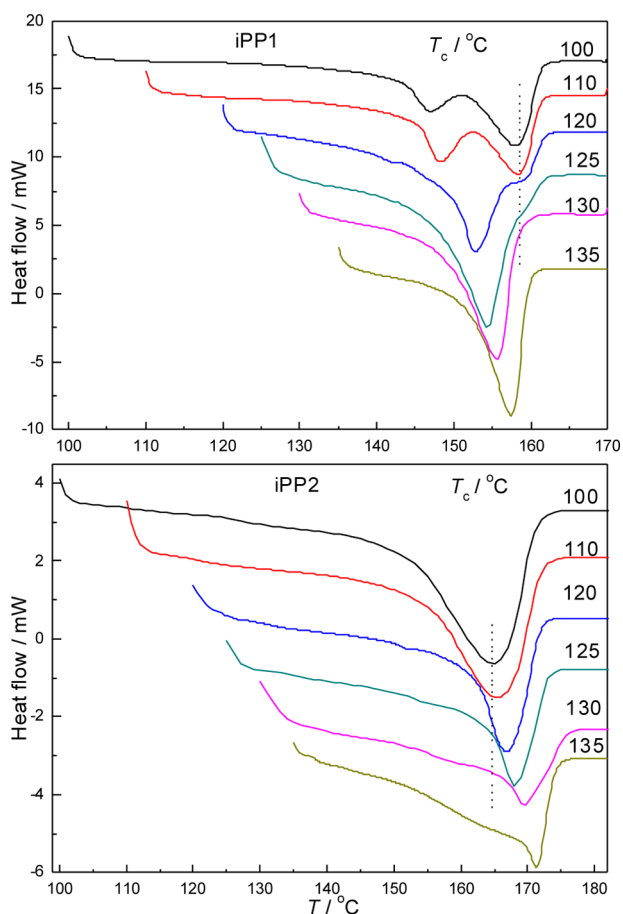


Figure 1. DSC melting curves of iPP1 (top) and iPP2 (bottom) measured after isothermal crystallization at the indicated temperatures in the plots (heating rate: 10 K/min).

Considering the melting behaviors can be affected by heating rate, annealing temperature, time, and so on,¹³ for minimizing the difference of melting behavior measured by DSC and SAXS techniques, the crystallization time for iPP samples used in DSC measurements was extended significantly to allow completion of crystalline perfection process. As it turned out, the iPP1 with lower molecular weight of 12000 g/mol showed two melting peaks when the crystallization temperature was below 130 °C. The higher melting peak can be apparently assigned to the melting of recrystallized crystallites during heating on account of its constant location, regardless of the crystallization temperature T_c .¹⁴ With the increase of T_c , the recrystallization process was suppressed, and therefore, only one melting peak was presented. This could be ascribed to the facts of a higher stability of the initial crystallites produced at higher T_c and less time left for recrystallization.¹⁴ The performance of the iPP2 with higher molecular weight of 340000 g/mol was different showing evidence of melting

directly without recrystallization during heating for samples crystallized at all temperatures. Obviously, the melting temperature for the two iPPs crystallized at same temperatures was different. It can thus be estimated that the molecular weight has an influence on the melting process.

In order to establish relationships between crystallization and melting temperatures and crystalline lamellar thickness, we performed in situ SAXS experiments during heating process of isothermally crystallized samples of both iPPs. Figure 2 presents

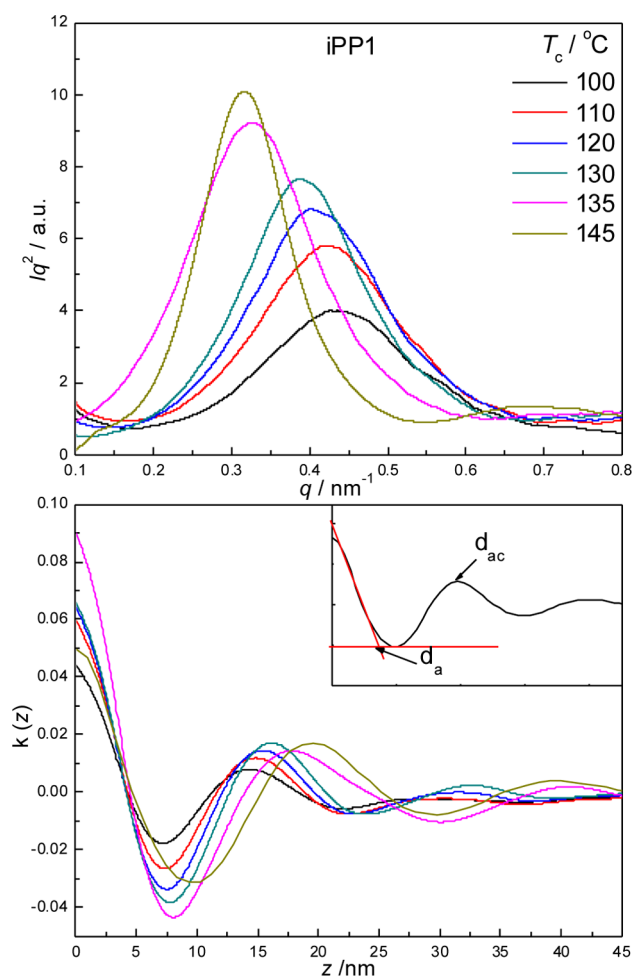


Figure 2. Selected one-dimensional scattering intensity distribution profiles (top) and the corresponding correlation function curves (bottom) of isothermally crystallized iPP1 at different temperatures. The inset presents the method of determining the thicknesses of amorphous layers, the long spacing, and crystalline lamellae.

selected one-dimensional SAXS profiles and their corresponding correlation function curves for iPP1 isothermally crystallized at different temperatures. During the whole crystallization and melting processes, only α crystalline modification develops in the current experimental T_c range, which is also evidenced by the absence of β phase melting peak around 155 °C¹⁵ in Figure 1, ensuring the suitability of using the correlation function approach to derive the thicknesses of amorphous layers (d_a), the long spacing (d_{ac}), and crystalline lamellae (d_c). Attributing to the weight crystallinities of both iPPs measured by DSC being more than 50% at any T_c the method of calculating the d_a , d_{ac} , and $d_c = d_{ac} - d_a$ was defined as shown in the inset of Figure 2.¹⁶ The evolution of the three parameters of both iPP1 and iPP2 all increased with elevating the T_c such general

properties have been often observed and reported on.^{17–19} According to the results derived from the correlation function curves, a diagram of the T_c and temperature T during subsequent heating process versus the d_c^{-1} is given in Figure 3. The main melting points derived from DSC curves in Figure

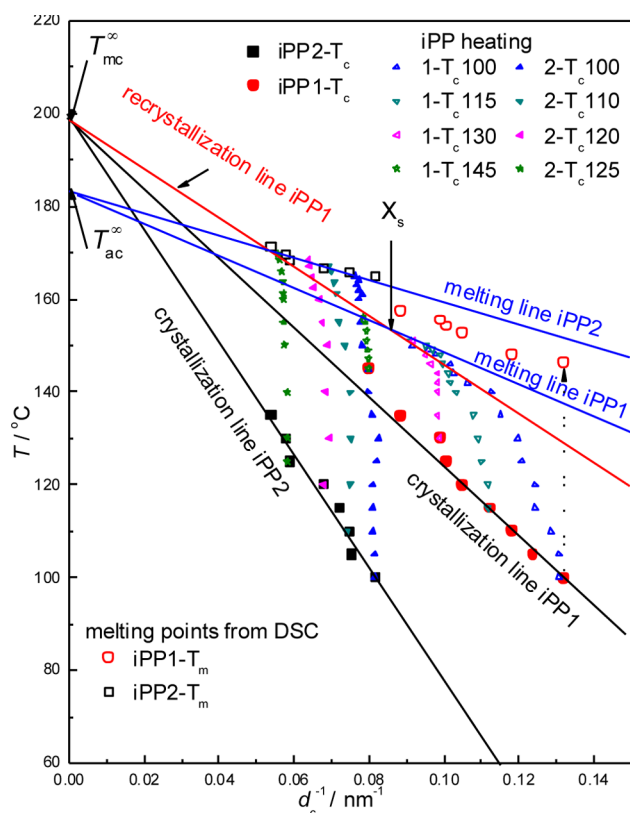


Figure 3. Relations between the d_c^{-1} and the T_c (crystallization lines), and T_m (melting line) of iPP1 and iPP2, and of two iPP samples during heating scans subsequent to isothermal crystallization at the indicated temperature T_c as derived from the temperature-dependent SAXS experiments.

I were also included. For iPP2, the DSC melting points agree very well with the ones determined by SAXS, whereas for iPP1 a systematic deviation was found that the DSC melting points are always higher than the SAXS ones. Such deviation might be caused by the influence of melting and recrystallization process during heating as the SAXS results showed that structural rearrangement occurred as soon as heating started.¹²

Clearly, the resultant linear dependencies of inversed lamellar thickness on crystallization temperature and melting temperature (i.e., crystallization line and melting line) confirm the recently developed multistage model for polymer crystallization by Strobl. Formation of final stabilized crystalline lamellae of polymers from molten state has been considered to proceed via several intermediate states.¹¹ The first step is always a creation of a mesomorphic phase that spontaneously thickens up to a critical thickness where it solidifies into a native crystalline block. The native crystalline blocks then merge together forming finally crystalline lamellae via stabilization process. Melting of the crystalline lamellae, however, goes via a direct route to an amorphous phase. In some cases, transition between stabilized crystalline phase to mesomorphic one can occur. The thus produced mesomorphic phase can spontaneously be transferred into stable crystalline phase of larger

thickness and higher stability. The process continues until a final melting is reached. Such process is known as a melting and recrystallization process during heating and is described by a recrystallization line in the above-mentioned phase diagram.¹¹ Support of such a view of polymer crystallization can be found directly from the phase diagram. First of all, the crystallization line does not overlap with the melting line indicating a nonreversible character of the processes. Second, the crystallization line is controlled by a limiting temperature for infinite lamellar thickness much higher than the one controlling the melting line. Thus, an introduction of the mesomorphic phase is mandatory. Therefore, the crystallization line, recrystallization line, and melting line in the multiage crystallization model can be described by three characteristic formulas:¹¹

The crystallization line:

$$T_{mc}^{\infty} - T \approx \frac{(2\sigma_{ac_n} - 2\sigma_{am})T_{mc}^{\infty} \Delta z}{\Delta H_{cm} d_c} \quad (1)$$

the recrystallization line:

$$T_{mc}^{\infty} - T \approx \frac{(2\sigma_{ac_s} - 2\sigma_{am})T_{mc}^{\infty} \Delta z}{\Delta H_{cm} d_c} \quad (2)$$

and the melting line:

$$T_{ac}^{\infty} - T \approx \frac{2\sigma_{ac_s} T_{ac}^{\infty} \Delta z}{\Delta H_{ca} d_c} \quad (3)$$

where ΔH_{cm} and ΔH_{ca} are the heats of transition from the mesomorphic phase to a crystalline phase and of the transition from the crystalline phase to the melt, Δz is the stem length increment per structural unit, and σ_{ac_n} , σ_{ac_s} , and σ_{am} denote the surface free energy of the native crystal layer, the stable crystal layer, and the mesomorphic layer, respectively.

With the help of above-mentioned laws, the different crystallization and melting behaviors presented in Figure 3 can be understood. In spite of giving two separated crystallization and melting lines between iPP1 and iPP2, they still shared the same equilibrium crystallization temperature T_{mc}^{∞} and equilibrium melting temperature T_{ac}^{∞} , and the differences exist only in the slope of their lines. According to eqs 1 and 2, it is clear that the cause of difference in slopes could be linked to the surface free energy since the other parameters remain unchanged. Apparently, the surface free energy difference of native crystallites and mesomorphic phase $\sigma_{ac_n} - \sigma_{am}$ increased with increasing molecular weight, whereas the surface free energy of stabilized crystallites σ_{ac_s} gave an opposite tendency being decreased with the increasing of molecular weight.

To understand the molecular weight dependencies of the surface free energies of native and stabilized crystallites in the iPP samples, a concept related to the morphology of chains in crystalline phase should be provided. The radius of gyration R_g of the chains in the melt is one evaluation for assuming the morphology of chains.⁷ Commonly, if the lamellar crystalline thickness d_c is smaller than R_g , the chains in crystallites exist as folded-chain state. But if d_c is larger than R_g , chains must be disentangled to certain extend leading to the formation of “extended-chain” crystals. Indeed, a change in the crystallization mechanism from folded-chain to extended-chain crystals has been observed in the different molecular weight PB-1s⁷ and PE_s.¹ Hence, we could use the same concept to explore the

chain morphology of the two iPPs. In the polymer melt R_g is obtained as follows:⁷

$$R_g^2 = \frac{R_0^2}{6} \quad (4)$$

and R_0 can be calculated via the characteristic ratio C_∞ as

$$R_0^2 = C_\infty a_b^2 N \quad (5)$$

where a_b^2 represents for the sum of the squares of the lengths of the backbone bonds of one monomer unit, and N is the degree of polymerization. In iPP, the values of C_∞ and a_b^2 are 5.8 and $4.74 \times 10^{-2} \text{ nm}^2$, correspondingly.¹⁸ And then by using the equations of 4 and 5, the values computed for R_g and d_c at different crystallization temperatures were summarized in Table 1.

Table 1. Radius of Gyration R_g Values of Two iPP Samples

name	M_w (kg/mol)	C_∞	a_b^2 (nm ²)	R_g (nm)	d_c (nm; 100–135 °C)
iPP1	12	5.8	4.74×10^{-2}	3.6	7.6–11.3
iPP2	340	5.8	4.74×10^{-2}	19.3	12.3–18.6

As it appeared, the iPP1 possessed the values of d_c much larger than R_g , while the iPP2 displayed the results of d_c smaller than R_g at all T_c s. The findings clearly indicate that the iPP1 developed native crystallites with extended-chain but the iPP2 formed native crystallites with folded-chain. It is aforementioned that the polymer with folded-chain crystallites has a crowded and disordered surface region resulting in a higher surface free energy.³ The iPP1 evidently ends the crystalline thickness close to the extended chain length, while the crystalline thickness in iPP2 is much smaller than the extended chain length. As a consequence, a lower surface free energy occurred in iPP1 resulting in a crystallization line for iPP1 with a smaller slope.

For the melting process, the surface free energy of stable crystallites showed a different response to the molecular weight compared to the surface free energy of native crystallite. Indeed, it has been reported that the surface free energy σ_e obtained from the Gibbs–Thomson equation slightly reduces with the increase of molecular weight in iPP attributing to the change in number of chain ends on the lamellar surfaces.⁵ Clearly, crystallites in iPP1 possess much more chain ends than that of iPP2 due to their extended-chain crystalline nature. During the heating process, the mobility devoted by chain ends in iPP1 was evidently more intensive than the one contributed by a large content of entanglement chains²¹ in iPP2, leading to a higher surface free energy of stable crystallites in iPP1 than the one in iPP2. Hence, the melting line of iPP1 exhibited larger slope than the one of iPP2. One important aspect should be referred to is that the isotacticity can also influence the surface free energy and thus the melting behavior.²² However, the two iPPs have the same isotacticity of 86% according to the nuclear magnetic resonance (NMR) results. Consequently, the effect of isotacticity was not in consideration in current case.

Here, one may notice the change of molecular weight dependency of surface free energy in iPP from the crystallization process to the melting course, such results agree with the crystallization model proposed by Strobl.¹¹ As the crystallization and melting processes proceed via different routes, the surface free energies in the two processes were controlled by different factors. Another feature of Figure 3

should be mentioned is the observed recrystallization process in iPP1 but not in iPP2. The intersection point of the melting line and the recrystallization line at a certain temperature and a certain value of the d_c^{-1} marks the end of the recrystallization behavior, which is defined as X_s .¹⁴ Above X_s the crystallites melt directly without changing their thickness. According to eq 2, which describes the recrystallization behavior, one expects a much smaller slope of the recrystallization line for iPP2 as the surface free energy of its stabilized crystallites is smaller than that of iPP1. Clearly, such recrystallization line would intersect with the melting line of iPP2 at a position of lamellar thickness smaller than observed here. The apparent discrepancy of recrystallization process in two iPPs can be associated with the crystallites stability. In iPP1, thin lamellae with lower stability can only be stabilized through growing thicker during heating via a melting and recrystallization process.¹³ On the other hand, in iPP2, the much thicker lamellae possess much higher stabilities that are stable during heating.¹² Such thicker crystallites can be melted at higher temperature,^{12,13} and accordingly, the recrystallization process would be suppressed.

In summary, the dependency of the molecular weight on the crystallization and melting behaviors were observed in the system of two iPPs. Differences in crystallization and melting processes for samples with different molecular weights can be understood as a consequence of changing in surface free energies of native and stabilized crystallites due to molecular weight. For native crystallites, the surface free energy increases with the increasing of molecular weight resulting in thicker crystalline lamellae for samples of higher molecular weight. During melting process, the surface free energy of stable crystallites decreases with the increasing of molecular weight. The phenomenon can be attributed to the fact that much more chain ends exist on the lamellar surfaces of low molecular weight sample.

EXPERIMENTAL SECTION

Two iPPs were purchased from Aldrich Polymer Products, being the iPP1 with a lower molecular weight of $M_w = 12000 \text{ g/mol}$ and a polydispersity (M_w/M_n) of 2.4, and the iPP2 with a higher molecular weight of $M_w = 340000 \text{ g/mol}$ and a polydispersity (M_w/M_n) of 3.5. The isotacticity of both samples is 86%, as was determined by ¹³C NMR measurements of their 1,2-dichlorobenzene-*d*₄ solutions at 125 °C. The pellets were molded in a hot press at 200 °C, developing films of 0.5 mm in thickness, and then rapidly transferred into a vacuum oven for isothermal crystallization at selected crystallization temperatures for time long enough (more than 12 h) to complete the crystallization. DSC measurements were carried out with a DSC1 Star^e System (Mettler Toledo Swiss) under N₂ atmosphere under a heating rate of 10 K/min. The samples for DSC measurements were isothermally crystallized for an extend time to account for the thermal annealing effect occurred during SAXS measurements. The ideal values of heat of fusion for 100% crystallinity of $\Delta H_{id} = 207 \text{ J g}^{-1}$ for iPP²⁰ was chosen to calculate the weight crystallinity. SAXS experiments were conducted with a modified Xeuss system of Xenocs, France at a sample-to-detector distance of 1063 or of 2450 mm. A multilayer focused Cu K α X-ray source (GeniX3D Cu ULD, Xenocs SA, France, $\lambda = 0.154 \text{ nm}$) and scatterless collimating slits were used during the experiments. SAXS images were recorded with a Pilatus 100 K detector of Dectris, Swiss. In situ SAXS measurements were performed during heating up the iPP1 and iPP2 samples from their isothermal crystallization temperatures to the molten state at a heating rate of 0.03 K/min. Each SAXS pattern was collected within 30 min which was then background corrected and normalized using the standard procedure.

AUTHOR INFORMATION

Corresponding Author

*E-mail: men@ciac.ac.cn.

Notes

The authors declare no competing financial interest.

ACKNOWLEDGMENTS

This work is supported by the National Natural Science Foundation of China (21134006).

REFERENCES

- (1) Devoy, C.; Mandelke, L. *J. Polym. Sci., Part A-2* **1969**, *7*, 1883–1894.
- (2) Schultz, J. M.; Robinson, W. H.; Pound, G. M. *J. Polym. Sci., Part A-2* **1967**, *5*, 511–533.
- (3) Mandelke, L.; Price, J. M.; Gopalan, M.; Fatou, J. G. *J. Polym. Sci., Part A-2* **1966**, *4*, 385–400.
- (4) Cheng, S. Z. D.; Janimak, J. J.; Zhang, A.; Cheng, H. N. *Macromolecules* **1990**, *23*, 298–303.
- (5) Yamada, K.; Hikosaka, M.; Toda, A.; Yamazaki, S.; Tagashira, K. *J. Macromol. Sci. Phys.* **2003**, *B42*, 733–752.
- (6) Kajioaka, H.; Yamada, K.; Taguchi, K.; Toda, A. *Polymer* **2011**, *52*, 2051–2058.
- (7) Fu, Q.; Heck, B.; Strobl, G.; Thomann, Y. *Macromolecules* **2001**, *34*, 2502–2511.
- (8) Cortazar, M.; Guzman, G. M. *Makromol. Chem.* **1982**, *183*, 721–729.
- (9) Wang, Y. T.; Lu, Y.; Jiang, Z. Y.; Men, Y. *Macromolecules* **2014**, *47*, 6401–6407.
- (10) Magill, J. H. *J. Polym. Sci., Part A-2* **1967**, *5*, 89–99.
- (11) Strobl, G. *Rev. Mod. Phys.* **2009**, *81*, 1287–1300.
- (12) Iijima, M.; Strobl, G. *Macromolecules* **2000**, *33*, 5204–5214.
- (13) Cheng, S. Z. D. *Phase Transitions in Polymers: The Role of Metastable States*; Elsevier Science: New York, 2008.
- (14) Al-Hussein, M.; Strobl, G. *Eur. Phys. J. E* **2001**, *6*, 305–314.
- (15) Lu, Y.; Wang, Q.; Men, Y. F. *J. Polym. Sci., Part B: Polym. Phys.* **2014**, *52*, 1301–1308.
- (16) Tanabe, Y.; Strobl, G. R.; Fischer, E. W. *Polymer* **1986**, *27*, 1147–1153.
- (17) Jiang, Z. Y.; Tang, Y. J.; Rieger, J.; Enderle, H. F.; Lilge, D.; Roth, S. V.; Gehrke, R.; Wu, Z. H.; Li, Z. H.; Men, Y. F. *Polymer* **2009**, *50*, 4101–4111.
- (18) Corneliu, R.; Peterlin, A. *Makromol. Chem.* **1967**, *105*, 193–203.
- (19) Heck, B.; Hugel, T.; Iijima, M.; Sadiku, E.; Strobl, G. *New J. Phys.* **1999**, *1*, 17.1–17.29.
- (20) Brandrup, J.; Immergut, E. H.; Grulke, E. A. P. *Polymer Handbook*, 4th ed.; John Wiley & Sons: New York, 2003.
- (21) Li, X. Y.; Ma, Z.; Su, F. M.; Tian, N.; Ji, Y. X.; Lu, J.; Wang, Z.; Li, L. B. *Chin. J. Polym. Sci.* **2014**, *32*, 1224–1233.
- (22) Cheng, S. Z. D.; Janimak, J. J.; Zhang, A. Q.; Hsieh, E. T. *Polymer* **1991**, *32*, 648–655.